





## A Novel SLM Scheme For Peak-To-Average Power Ratio Reduction In WOLA-OFDM System

### WOLA-OFDM Sisteminde Tepe Gücü/Ortalama Güç Oranının Düşürülmesi İçin Yeni Bir SLM Şeması

<sup>1</sup>Sakir ŞİMŞİR , <sup>2</sup>Necmi TAŞPINAR 

<sup>1</sup>Nevşehir Hacı Bektaş Veli University, Department of Electrical and Electronics Engineering, Nevşehir, Türkiye

<sup>2</sup>Erciyes University, Department of Electrical and Electronics Engineering, Kayseri, Türkiye

<sup>1</sup>sakirsimsir@nevsehir.edu.tr, <sup>2</sup>taspinar@erciyes.edu.tr

Araştırma Makalesi/Research Article

#### ARTICLE INFO

##### Article history

Received : 27 May 2024

Accepted : 25 June 2024

##### Keywords:

PAPR, Selective Mapping,  
WOLA-OFDM, Dual Symbol  
Optimization, 5G

#### ABSTRACT

This paper addresses high peak-to-average power ratio (PAPR) issue in the recently invented weighted overlap and add-orthogonal frequency division multiplexing (WOLA-OFDM) system. The selective mapping (SLM), one of the most widely used PAPR reduction schemes in OFDM-based multicarrier transmission strategies, can be used to reduce the PAPR of WOLA-OFDM signals. However, the overlapping of symbol extensions in the WOLA-OFDM transmitter considerably deteriorates the performance of SLM. To overcome this problem, we have developed an efficient SLM scheme named dual symbol optimization-SLM (DSO-SLM) for the WOLA-OFDM system. In this new scheme, instead of reducing the PAPR of adjacent symbols separately as in conventional SLM, each symbol is evaluated together with its overlapping predecessor symbol while searching for the optimal transmission signal with minimized PAPR. With the usage of DSO procedure, it becomes possible to enhance the performance of conventional SLM in the WOLA-OFDM system.

© 2024 Bandırma Onyedi Eylül University, Faculty of Engineering and Natural Science. Published by Dergi Park. All rights reserved.

#### MAKALE BİLGİSİ

##### Makale Tarihleri

Gönderim : 27 Mayıs 2024

Kabul : 25 Haziran 2024

##### Anahtar Kelimeler:

PAPR, Seçici Eşleme, WOLA-OFDM, Çift Sembol Optimizasyonu, 5G

#### ÖZET

Bu makale, yakın zamanda bulunan ağırlıklı örtüşürme ve ekleme-dikgen frekans bölmeli çoğullama (WOLA-OFDM) sistemindeki yüksek tepe gücü/ortalama güç oranı (PAPR) sorununu ele almaktadır. OFDM tabanlı çok taşıyıcı iletim stratejilerinde en yaygın kullanılan PAPR düşürme şemalarından biri olan seçici eşleme (SLM), WOLA-OFDM sinyallerinin PAPR değerini düşürmek için kullanılabilir. Ancak, WOLA-OFDM vericisinde sembol uzantılarının örtüşmesi, SLM'nin performansını önemli ölçüde kötüleştirmektedir. Bu sorunun üstesinden gelmek amacıyla, WOLA-OFDM sistemi için, çift sembol optimizasyon tabanlı SLM (DSO-SLM) isimli etkili bir SLM şeması geliştirdik. Bu yeni şemada, geleneksel SLM'de olduğu gibi komşu sembollerin PAPR değerini ayrı ayrı düşürmek yerine, PAPR değeri minimize edilmiş optimum iletim sinyali aranırken her bir sembol, kendisiyle örtüşen bir önceki sembol ile birlikte değerlendirilmektedir. DSO prosedürünün kullanımıyla birlikte, geleneksel SLM'nin WOLA-OFDM sistemindeki performansını artırmak mümkün hale gelmektedir.

© 2024 Bandırma Onyedi Eylül Üniversitesi, Mühendislik ve Doğa Bilimleri Fakültesi. Dergi Park tarafından yayınlanmaktadır. Tüm Hakları Saklıdır.

ORCID ID: <sup>1</sup>0000-0002-1287-160X  
<sup>2</sup>0000-0003-4689-4487

## **1. INTRODUCTION**

Over the last years, a life without internet has almost become unthinkable. It has become an integral part of our daily life with especially the widespread use of smartphones and the other mobile internet-based smart devices. Some mobile applications such as video conferencing, e-healthcare, video streaming and online gaming, each of which can be utilized regardless of place and time in a day, has now become regular services. Such a dramatic enhancement in the usage of smartphone and accordingly the mobile internet unavoidably has caused the mobile data traffic to reach an unprecedented level. Moreover, the technologies like machine type communication (MTC) and internet of things (IoT), which are now gradually becoming wide spread and expected to make our lives easier in the future, are going to add extra load to the current mobile data traffic that has already reached very high levels and barely been supported by the current cellular systems [1-3].

In order to cope with the aforementioned exponential growth in the mobile data traffic and provide smooth communication between the growing number of subscribers using mobile internet together with the millions of electronic devices and objects connected to each other, the new waveforms have been developed to be utilized in the fifth generation (5G) and beyond telecommunication technologies [4]. Weighted overlap and add-orthogonal frequency division multiplexing (WOLA-OFDM) [5] is one of the related new generation waveforms. The unique features that WOLA-OFDM has make it to be considered among the promising waveform candidates likely to be employed in the future telecommunication technologies in place of the conventional OFDM utilized in the current cellular systems. In the WOLA-OFDM system, the signal obtained right after the addition of cyclic prefix is expanded in the time domain. Later on, the windowing operation applied to the expanded signal to make it ready for the transmission. In the WOLA-OFDM, thanks to the quite simple and very effective time domain windowing operation, the out of band radiation can be suppressed in a powerful way. Apart from this, being resistant to the problem of asynchronism in the users and having a structure suitable for multiple-input multiple-output (MIMO) implementations consolidate the WOLA-OFDM's place among the 5G and beyond waveform candidates [5-8].

### **1.1. Motivation**

On the other hand, as in the traditional OFDM, WOLA-OFDM suffers from the problem of high peak-to-average ratio (PAPR) as well. The PAPR value is measured on the transmission signal. What makes the transmission signal to have high PAPR value in such waveforms is the formation of momentary power spikes resulting from the combination of multiple subcarriers. The main reason making it a real problem that the transmission signals have high PAPR values is the necessity of amplifying them via a nonlinear high-power amplifier (HPA) [9,10] prior to the transmission process. The transmission signals with high power peaks, which result in high PAPR value as well, make such amplifiers to reach saturation region where the amplification process is carried out in an unhealthy way by causing considerable deformations on the signals to be amplified. In order to prevent the transmission signals from being distorted by the nonlinear HPAs, their PAPR values have to be kept at low levels. To this end, the researchers have proposed assorted PAPR lowering strategies in the literature [11,12].

Selective mapping (SLM) is a popular and one of the prominent PAPR lowering strategies existing in the literature due to its superior features [13,14]. Thanks to the strategy of phase rotation used in the SLM scheme, PAPR alleviation in the transmission signals can be carried out without leading to any loss of information. Another advantageous attribute that augments the frequentness of SLM usage in different transmission technologies is its flexible structure, which is appropriate for the operations of both modification and hybridization. It is possible to exploit such advantageous features that SLM has in the WOLA-OFDM waveform as well. However, since the SLM method is originally designed for the conventional OFDM in the first place, direct application of the relevant method to the transmitter of WOLA-OFDM will prevent it from reaching its full potential. Because, prior to the transmitting operation of the WOLA-OFDM system, right after the symbols are extended from their beginnings and ends, excluding the first symbol, the beginning appendage of each symbol is allowed to overlap with the end appendage of the preceding symbol, whereas the symbols are transmitted independently without any overlapping operation in the classical OFDM system. Therefore, even though the PAPR of related symbols are lowered individually as in the classical SLM method, the PAPR regrowth will happen in the signal obtained following the overlapping process. In this paper, for the purpose of eliminating the PAPR re-growth arising from the symbol overlapping implementation, dual symbol optimization-based SLM (DSO-SLM) strategy was developed for the WOLA-OFDM system by modifying the traditional SLM method. In our suggested DSO-SLM technique, unlike the classical SLM, in which every symbol is optimized independently, the PAPR reduction is carried out by evaluating each symbol together with the previous neighboring symbol whose end extension is overlapped with the beginning extension of the current symbol being optimized. In this way, the capability of SLM to reduce PAPR in the WOLA-OFDM waveform has been boosted by eliminating the adverse impact of the overlapping of adjacent symbols.

### **1.2. Related Works**

When examining the literature carefully, it is seen that there are only three studies related to PAPR reduction in the WOLA-OFDM waveform [15-17]. That is a pretty low number and further studies are needed in this field. The

mentioned studies are as follows: In [15], the PAPR alleviation performances of the SLM and tone reservation (TR) techniques were analyzed in not only WOLA-OFDM, but also two different 5G waveform candidates called filtered-OFDM (f-OFDM) and universal filtered multicarrier (UFMC), respectively. In [16], SLM and TR-based PAPR reduction operations were carried out as in the study numbered [15]. But this time, as well as the WOLA-OFDM, a special waveform named block filtered-OFDM (BF-OFDM) was handled. Aforementioned PAPR reduction techniques and their modified versions developed for the BF-OFDM waveform were applied together with the digital predistortion operation for the purpose of increasing the energy efficiency and avoiding the non-linear degradations created by the high-power amplifier. In [17], the authors integrated the procedure of dual symbol optimization, which was originally developed in the same study, to the classical partial transmit sequence (PTS) scheme to create more efficient PAPR lowering method named DSO-PTS for the WOLA-OFDM scheme.

### 1.3. Contributions

Our study provides the following contributions to the literature:

- 1) It is the first time in the literature to combine the dual symbol optimization procedure with the traditional SLM to create a new PAPR lowering strategy named DSO-SLM for the WOLA-OFDM waveform.
- 2) A significant improvement has been achieved in the performance of classical SLM after being combined with the mechanism of dual symbol optimization.
- 3) The proposed DSO-SLM technique not only outperforms the conventional SLM scheme, but also leaves behind two efficient benchmark strategies called GreenOFDM [18] and DSO-PTS considered for comparison in this paper.

*Paper organization:* The WOLA-OFDM transmitter and receiver structures are explained in Section 2. The PAPR definition for the WOLA-OFDM signal is carried out in Section 3. The classical SLM technique is described in Section 4. The suggested DSO-SLM scheme is described in detail along with its operating steps in Section 5. Simulation results are yielded in Section 6 and finally, the paper is concluded in Section 7.

## 2. EXPLANATION OF WOLA-OFDM TRANSCEIVER

The WOLA-OFDM structure is illustrated in Figure 1. The processing blocks encircled by the dashed lines are special to the WOLA-OFDM scheme. Figure 2 and Figure 3 visualize the WOLA process represented by these operation blocks at the transmitter and receiver, respectively [5-8]. In these figures,  $E$  and  $P$  indicate the lengths of overlap extension and cyclic prefix, respectively. In WOLA-OFDM, the disadvantage of using a rectangular

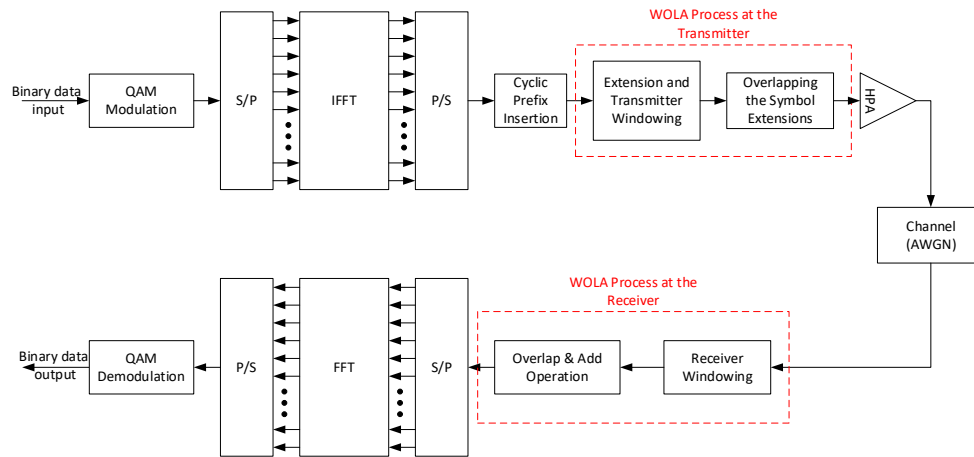


Figure 1. The WOLA-OFDM transceiver structure.

shaped pulse leading to spectral regrowth in the conventional OFDM is eliminated via multiplying the contiguous symbols in time domain by a soft-edged windowing function. By doing so, soft transitions are obtained in the time domain symbols and in consequence of this, a significant suppression is achieved in the out of band emission.

The operations peculiar to WOLA-OFDM transmitter can be seen from the Figure 2. As can be easily grasped from that figure,  $(P + E)$ -length piece of time domain symbol with the length  $N$  is duplicated from the end of the related symbol and then attached to its beginning. Afterward,  $E$ -length piece of the  $N$ -length symbol is copied from its beginning and then added to its end to complete the operation of symbol extension, in which the symbol length is increased from the value of  $N$  to  $(N + P + 2E)$ . Following the termination of symbol extension procedure, the windowing operation is put into practice on the extended signals. Later on, the contiguous signals windowed one by one in the previous stage are overlapped from their overlap extensions. The overlapping operation makes it possible to equalize the overhead of WOLA-OFDM signal with that of the classical OFDM signal. To put it more clearly, the period increase arising from the extra  $E$ -length extensions in the time domain symbols can be avoided through the overlapping operation. Therefore, the decrease of signal rate due to the period increase can be

prevented as well. After finishing the overlapping operation, the resulting WOLA-OFDM signal is made ready for the transmission by amplifying it via a high-power amplifier.

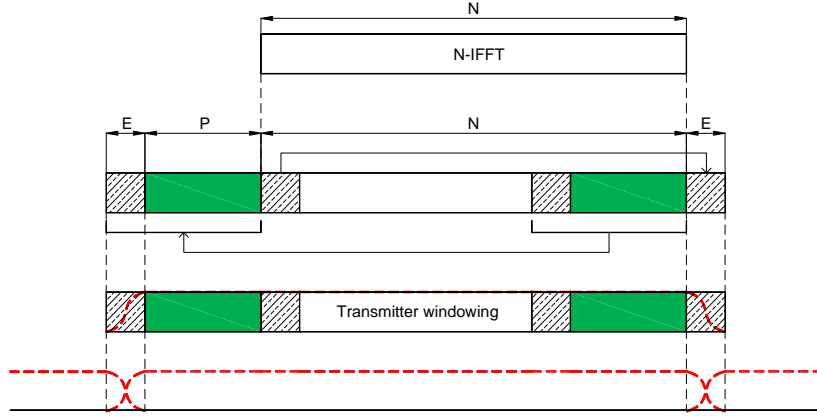


Figure 2. The transmitter side WOLA operations.

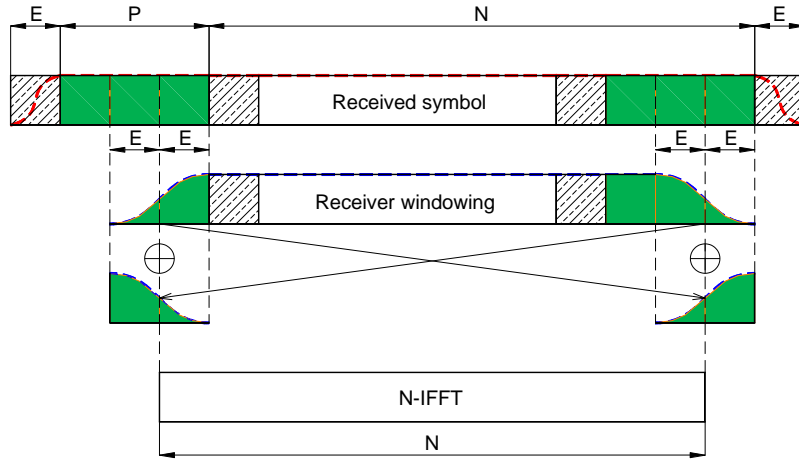


Figure 3. The receiver side WOLA operations.

In Figure 3, the visual explanation of the WOLA operations carried out at the receiver side is given. As shown in Figure 3, WOLA process is performed at the receiver side as well for the purpose of suppressing the asynchronous inter-user interference. As can be noticed from the Figure 3, the receiver window length is equal to  $(N + 2E)$  while the length of the transmitter window is  $(N + P + 2E)$ . Besides, the transition regions of the receiver window are  $2E$  long while those of the transmitter window have the length of  $E$ . Subsequent to the receiver side windowing operation, the process of overlap and add is carried out to recover the information data from the windowing effects and after all,  $N$ -length symbol is acquired at the receiver side [5-8].

### 3. DEFINITION OF PAPR FOR WOLA-OFDM WAVEFORM

In order to make PAPR definition in WOLA-OFDM waveform, it is required to acquire the mathematical expression of the transmission signal. To this end, in the first place, the OFDM signal is defined in continuous time as follows [17]:

$$x_m(t) = \frac{1}{\sqrt{N}} \sum_{k=0}^{N-1} X_{m,k} e^{j2\pi f_k t}, 0 \leq t \leq NT, 1 \leq m \leq M \quad (1)$$

where  $x_m(t)$  represents the complex envelope of the  $m$ th OFDM symbol while  $X_{m,k}$  denotes the  $k$ th symbol of the  $m$ th quadrature amplitude modulation (QAM) symbol vector.  $f_k$  is the subcarrier frequency appointed to the  $k$ th QAM symbol.  $T$  is the symbol period and  $N$  is the subcarrier number. The studies on PAPR reduction are practically performed on discrete signals. For this reason, the discrete-time expression of the  $m$ th OFDM symbol is acquired by implementing  $L$ -factor oversampling operation in the following way [17]:

$$x_m[n] = \frac{1}{\sqrt{N}} \sum_{k=0}^{N-1} X_{m,k} e^{j\frac{2\pi kn}{LN}}, 0 \leq n \leq LN - 1, 1 \leq m \leq M \quad (2)$$

when obtaining the signals in discrete-time, it is crucial to specify the factor of oversampling as  $L \geq 4$  [19] to get closer PAPR results to those of the original signals in continuous time. Following the oversampling process, each  $LN$ -length symbol vector is stretched to the length  $(LN + P + 2E)$  via the operations of appending cyclic prefix and overlapping extension, respectively. The expression given below defines the  $m$ th WOLA-OFDM symbol achieved subsequent to the aforementioned operations [17]:

$$y_m[n] = [x_m[LN - P - E], x_m[LN - P - E + 1], \dots, x_m[LN - 1], x_m[0], x_m[1], \dots, x_m[LN - 1], x_m[0], x_m[1], \dots, x_m[E - 1]], 0 \leq n \leq 2E + P + LN - 1 \quad (3)$$

The extended symbols obtained as a result of the completion of symbol extension process are subjected to the windowing operation via the flat-top root-raised-cosine (rrc) function acquired by benefiting from the square-root of the raised-cosine (Hann) windowing function [20]. The related Hann and flat top rrc windowing functions are formulated in Equation (4) and Equation (5), respectively [17]:

$$w[n] = \sqrt{\frac{1}{2} \left[ 1 - \cos\left(\frac{2\pi n}{N-1}\right) \right]}, 0 \leq n \leq N-1 \quad (4)$$

$$w[n] = \begin{cases} \sqrt{\frac{1}{2} \left[ 1 - \cos\left(\frac{\pi n}{E-1}\right) \right]}, & 0 \leq n \leq E-1 \\ 1, & E \leq n \leq E + P + LN - 1 \\ \sqrt{\frac{1}{2} \left[ 1 + \cos\left(\frac{\pi[n - (E + P + LN)]}{E-1}\right) \right]}, & E + P + LN \leq n \leq 2E + P + LN - 1 \\ 0, & \text{for the other } n \text{ values} \end{cases} \quad (5)$$

The operation of windowing is fulfilled through the multiplication of prolonged symbols expressed in Equation (3) by the windowing function defined in Equation (5) as follows [17]:

$$s_m[n] = w[n]y_m[n], 0 \leq n \leq 2E + P + LN - 1 \quad (6)$$

where  $s_m[n]$  represents the  $m$ th symbol windowed by the flat top rrc function. After the termination of windowing implementation, the extensions of the symbol vectors are overlapped as illustrated in Figure 4.

The mathematical expression of WOLA-OFDM transmission signal obtained as a result of overlapping operation is given below [17]:

$$s[n] = \sum_{m=1}^M s_m[n - (m-1)(E + P + LN)], 0 \leq n \leq M(P + LN + E) + E - 1 \quad (7)$$

Finally, the PAPR definition for the WOLA-OFDM transmitting signal is performed as follows [17]:

$$PAPR(s[n]) = 10 \log_{10} \frac{\max_{0 \leq n \leq M(P+LN+E)+E-1} [|s[n]|^2]}{E[|s[n]|^2]} \text{ (dB)} \quad (8)$$

#### 4. CLASSICAL SLM TECHNIQUE

Figure 5 is the demonstration of how the PAPR alleviation is put into practice via the conventional SLM scheme. As explicitly viewed from the Figure 5, in the classical SLM technique, the first operation is to produce  $U$  copies of vector  $X = [X_0, X_1, \dots, X_{K-1}]$  given to the SLM input. Later on,  $K$ -length random phase sequence defined in the following equation is generated for each of the resulting vector copies [13,14].

$$b^{(u)} = [b_0^{(u)}, b_1^{(u)}, \dots, b_{K-1}^{(u)}], u = 0, 1, \dots, U - 1 \quad (9)$$

In the equation above,  $b_k^{(u)} \in \{-1, +1\}$  where  $k = 0, 1, \dots, K - 1$ . These phase sequences having the same length with the vector  $X$  are then multiplied by the copies of the related  $X$  vector in an element-wise manner to execute the phase rotation process in the following way [13,14]:

$$X^{(u)} = [X_0 \cdot b_0^{(u)}, X_1 \cdot b_1^{(u)}, \dots, X_{K-1} \cdot b_{K-1}^{(u)}] = [X_0^{(u)}, X_1^{(u)}, \dots, X_{K-1}^{(u)}] \quad (10)$$

where the data vector  $X^{(u)}$  achieved through the multiplication of  $b_k^{(u)}$ ,  $b_k^{(u)}$  by the vector  $X$  denotes the phase-rotated  $u$ th data sequence. Subsequently, the resulted  $X^{(u)}$  vectors are subjected to the addition of  $(L - 1) \cdot K$  zeros and inverse fast Fourier transform (IFFT) operations, respectively to attain their time domain versions oversampled by the factor  $L$  as follows [13,14]:

$$x^{(u)}[n] = IFFT(X^{(u)}) = \frac{1}{\sqrt{K}} \sum_{k=0}^{K-1} X_k \cdot b_k^{(u)} \cdot e^{j\frac{2\pi kn}{LK}}, 0 \leq n \leq LK - 1 \quad (11)$$

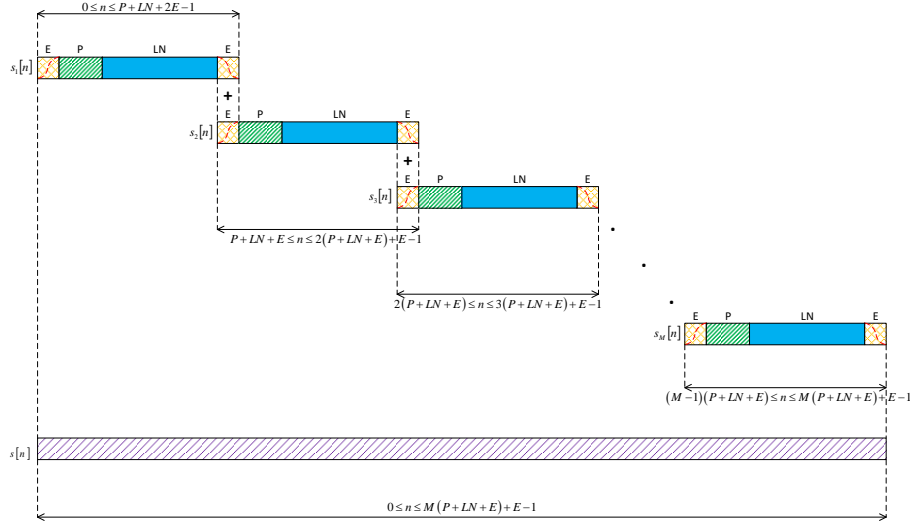


**Figure 4.** The process of overlapping the symbol vectors in WOLA-OFDM.

After that, in order to determine which of the candidate signals indicated by  $x^{(u)}[n]$  has the minimal PAPR value, PAPR of each one is calculated. Eventually, the candidate signal with the smallest PAPR, which is symbolized by  $x'[n]$  in Figure 5, is selected for transmission while the phase sequence leading to the production of that candidate signal is appointed as the optimal phase vector [13,14].

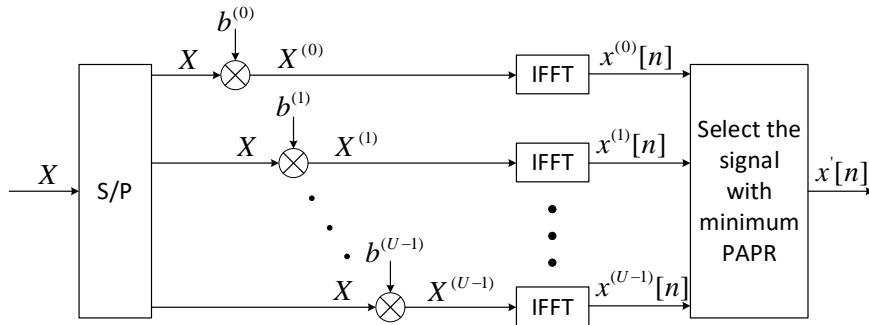


**Figure 5.** Classical SLM scheme.

### 5. THE PROPOSED DSO-SLM STRATEGY

In the classical SLM scheme, PAPR lowering is carried out by evaluating the contiguous symbols independently of each other. The aforementioned individual PAPR reduction strategy causes the related scheme to show quite poor performance when being applied directly to the WOLA-OFDM transmitter without any modification. Because, as mentioned before, no matter how much the PAPR value of each individual symbol is alleviated, PAPR growths will occur again in the WOLA-OFDM transmission signal acquired as a result of overlapping the related symbols from their extension parts. To avoid this undesired situation and obtain much better PAPR reduction performance, dual symbol optimization procedure, which was proposed in [17] to remove the PAPR enhancing impact of the overlapping operation, was combined with the traditional SLM scheme. In consequence of this combination process, a novel PAPR lowering scheme named DSO-SLM has been created for the WOLA-OFDM waveform. The steps of PAPR alleviation using DSO-SLM in WOLA-OFDM are as follows:

**Step 1:** The PAPR reduction process via DSO-SLM strategy starts with optimizing the first WOLA-OFDM symbol expressed by  $s_1[n]$ . To this end, at the beginning,  $U$  number of phase sequences differing from each other are generated, randomly for the first QAM symbol vector represented by  $X_1 = [X_{1,0}, X_{1,1}, \dots, X_{1,N-1}]$ . The aforementioned phase sequences are defined as follows:

$$b_1^{(u)} = [b_{1,0}^{(u)}, b_{1,1}^{(u)}, \dots, b_{1,N-1}^{(u)}], u = 0, 1, \dots, U - 1 \tag{12}$$

where each phase factor takes a maximum of two different values as  $b_m^{(u)} \in \{-1, +1\}$ . After that, the randomly generated phase sequences and the vector  $X_1$  are multiplied as follows:

$$X_1^{(u)} = [X_{1,0} \cdot b_{1,0}^{(u)}, X_{1,1} \cdot b_{1,1}^{(u)}, \dots, X_{1,N-1} \cdot b_{1,N-1}^{(u)}] = [X_{1,0}^{(u)}, X_{1,1}^{(u)}, \dots, X_{1,N-1}^{(u)}] \tag{13}$$

where the multiplication of  $X_1$  by the  $b_1^{(u)}$  corresponding to the  $u$ th randomly generated phase sequence gives the  $u$ th phase-rotated data vector denoted by  $X_1^{(u)}$ . The resulted  $X_1^{(u)}$  vector is then converted to time domain via

the IFFT process together with the  $L$ -factor oversampling operation as follows:

$$x_1^{(u)}[n] = \frac{1}{\sqrt{N}} \sum_{k=0}^{N-1} X_{1,k}^{(u)} e^{j\frac{2\pi kn}{LN}}, 0 \leq n \leq LN - 1, u = 0, 1, \dots, U - 1 \quad (14)$$

**Step 2:** In consequence of adding the cyclic prefix and overlapping extensions to the signal  $x_1^{(u)}[n]$ , the following signal is obtained:

$$y_1^{(u)}[n] = [x_1^{(u)}[LN - P - E], x_1^{(u)}[LN - P - E + 1], \dots, x_1^{(u)}[LN - 1], x_1^{(u)}[0], x_1^{(u)}[1], \dots, x_1^{(u)}[LN - 1], x_1^{(u)}[0], x_1^{(u)}[1], \dots, x_1^{(u)}[E - 1]], 0 \leq n \leq 2E + P + LN - 1 \quad (15)$$

The first WOLA-OFDM symbol  $s_1^{(u)}[n]$  is acquired by windowing the signal  $y_1^{(u)}[n]$ , which is acquired after the symbol extension process, with the help of flat top rrc function as follows:

$$s_1^{(u)}[n] = w[n]y_1^{(u)}[n], 0 \leq n \leq 2E + P + LN - 1 \quad (16)$$

**Step 3:** The optimum phase sequence  $b_1^*$  is determined for the first symbol of WOLA-OFDM as follows:

$$b_1^* = \arg \min_{b_1^{(u)}} \left\{ \max_{0 \leq n \leq 2E + P + LN - 1} |s_1^{(u)}[n]|^2 \right\} \quad (17)$$

**Step 4:** The optimized first WOLA-OFDM symbol expressed as  $s_1^*[n]$  is obtained by utilizing the optimum phase sequence  $b_1^*$  determined in the previous step as below:

$$X_1^* = [X_{1,0} \cdot b_{1,0}^*, X_{1,1} \cdot b_{1,1}^*, \dots, X_{1,N-1} \cdot b_{1,N-1}^*] = [X_{1,0}^*, X_{1,1}^*, \dots, X_{1,N-1}^*] \quad (18)$$

$$x_1^*[n] = \frac{1}{\sqrt{N}} \sum_{k=0}^{N-1} X_{1,k}^* e^{j\frac{2\pi kn}{LN}}, 0 \leq n \leq LN - 1 \quad (19)$$

$$y_1^*[n] = [x_1^*[LN - P - E], x_1^*[LN - P - E + 1], \dots, x_1^*[LN - 1], x_1^*[0], x_1^*[1], \dots, x_1^*[LN - 1], x_1^*[0], x_1^*[1], \dots, x_1^*[E - 1]], 0 \leq n \leq 2E + P + LN - 1 \quad (20)$$

$$s_1^*[n] = w[n]y_1^*[n], 0 \leq n \leq 2E + P + LN - 1 \quad (21)$$

**Step 5:** The second WOLA-OFDM symbol indicated by  $s_2^{(u)}[n]$  is acquired by re-performing the operations in Steps 1 and 2 for the second QAM vector expressed as  $X_2 = [X_{2,0}, X_{2,1}, \dots, X_{2,N-1}]$ .

**Step 6:** Taking into account that the right extension of the previous optimized symbol  $s_1^*[n]$  overlaps with the left extension of the symbol  $s_2^{(u)}[n]$  currently being optimized, the optimal phase vector  $b_2^*$  is obtained for the second symbol  $s_2^{(u)}[n]$  in the following manner:

$$b_2^* = \arg \min_{b_2^{(u)}} \left\{ \max_{E + P + LN \leq n \leq 2(E + P + LN) + E - 1} |s_1^*[n] + s_2^{(u)}[n - (E + P + LN)]|^2 \right\} \quad (22)$$

**Step 7:** The operations of Step 4 is reiterated for the second symbol to acquire  $s_2^*[n]$  corresponding to the optimized version of the second WOLA-OFDM symbol.

**Step 8:** The optimization of contiguous symbols is maintained in this way till the  $M$ th symbol one by one. The optimal phase vector for the  $M$ th symbol is determined in the following way:

$$b_M^* = \arg \min_{b_M^{(u)}} \left\{ \max_{(M-1)(P+LN+E) \leq n \leq M(P+LN+E) + E - 1} |s_{M-1}^*[n - (M-2)(E + P + LN)] + s_M^{(u)}[n - (M-1)(E + P + LN)]|^2 \right\} \quad (23)$$

**Step 9:** At last, the transmission signal with minimal PAPR is achieved through the summation of  $M$  number of optimized symbols by ensuring that the extension parts of the contiguous symbols are overlapped with each other as formulated below:

$$s^*[n] = \sum_{m=1}^M s_m^*[n - (m-1)(E + P + LN)], 0 \leq n \leq M(P + LN + E) + E - 1 \quad (24)$$

## 6. SIMULATION RESULTS

In this section, the performance gain of the DSO-SLM strategy over the traditional SLM scheme was investigated. For that purpose, the classical SLM was used as a benchmark strategy. Furthermore, the two SLM-based modified PAPR reduction strategies called GreenOFDM [18] and DSO-PTS [17], both of which have been proposed in recent years, were employed for comparison as well. The comparisons of the aforementioned PAPR reduction

strategies were put into practice based on the PAPR achievement and power spectral density (PSD) performance, which are the two main performance criteria frequently used in the PAPR reduction studies. In the classical PTS or its modified versions like DSO-PTS, in each search carried out for any of the WOLA-OFDM symbols, a random phase sequence expressed as  $b_m^{(v)} = [b_m^{(0)}, b_m^{(1)}, \dots, b_m^{(V-1)}]$  is generated and the total number of phase sequences generated, randomly is equal to the total number of searches denoted by  $SN$  parameter. In the conventional SLM, GreenOFDM, which is a type of modified SLM, and DSO-SLM techniques, the phase sequences generated for any WOLA-OFDM symbol is defined as  $b_m^{(u)} = [b_{m,0}^{(u)}, b_{m,1}^{(u)}, \dots, b_{m,N-1}^{(u)}]$ , and as in the PTS-based PAPR lowering schemes, a random phase sequence is generated for each search. However, unlike the PTS-based schemes, this time, the total number of phase sequences is determined by the  $U$  parameter. In other words, in the PAPR lowering studies based on SLM, the number of searches ( $SN$ ) becomes equal to  $U$  as  $SN = U$ . In this section, with a view to prevent any confusion in the comparisons to be made between the SLM and PTS-based PAPR lowering schemes for varied search numbers, when expressing the number of searches for the relevant schemes, only the parameter  $SN$  will be used. The values of parameters belonging to the simulation studies are given in Table 1.

**Table 1.** Simulation parameters.

<b>Size of FFT</b>	256
<b>HPA model</b>	SSPA
<b>Number of subcarriers</b>	$N = 32$
<b>Type of modulation</b>	4-QAM
<b>Number of symbols</b>	$M = 16$
<b>Cyclic prefix length</b>	$P = 24$
<b>Overlapping extension length</b>	$E = 8$
<b>Window type</b>	Flat top rrc window
<b>Channel model</b>	AWGN
<b>Value of oversampling factor</b>	$L = 8$
<b>DSO-PTS subblock number</b>	$V = 16$

In Figure 6, with the aim of observing how the variation of search number affects the PAPR lowering achievement of the DSO-SLM strategy, the value of parameter  $SN$  was increased, gradually from 4 to 256. The improvement in the performance of DSO-SLM due to the aforementioned gradual increment in the value of  $SN$  is evidently seen from the Figure 6. As can be viewed from the related figure, the more the search number is increased, the more the PAPR of the original signal improves. Because, the selection of a large  $SN$  value leads to the generation of more phase sequences and accordingly the production of more alternative transmission signals. With the increase in the alternative transmission signals, since the probability of obtaining a signal with a lower PAPR value will increase, the increment in the value of  $SN$  will make the performance of DSO-SLM to increase as well. In the Figure 6, the PAPR values acquired by the DSO-SLM at  $CCDF = 10^{-3}$  for  $SN = 4, 16, 64$  and  $256$  number of searches are equal to  $8.31$  dB,  $6.83$  dB,  $6.04$  dB and  $5.52$  dB, respectively. Note that  $CCDF$  is the complementary cumulative distribution function, which is defined as  $\Pr[PAPR > PAPR_0]$ .

In Figure 7,  $PAPR_0$  [dB] –  $CCDF$  curves of DSO-SLM, GreenOFDM and SLM techniques were obtained for both 32 and 64 number of searches. As it is obvious in the Figure 7, while doubling the number of searches results in PAPR improvement in each technique to a certain extent, DSO-SLM has been the best performing strategy that reaches the lowest PAPR level by making big differences to the GreenOFDM and SLM methods for both of the search numbers. For example, in case of taking  $CCDF = 10^{-3}$  as the point of reference, while the SLM and GreenOFDM methods reach  $7.96$  dB and  $7.48$  dB PAPR values, respectively for 32 searches, the DSO-SLM technique reaches  $6.37$  dB PAPR level by making  $1.59$  dB and  $1.11$  dB differences to the related methods for the same number of searches. Another point catching the eye in the Figure 7 is that the method achieving the highest amount of improvement with the rise of  $SN$  is the DSO-SLM method as well. This causes the DSO-SLM technique to widen the difference with the other methods even more as the value of  $SN$  is increased. For instance, while the difference of PAPR between the DSO-SLM and SLM at  $CCDF = 10^{-3}$  becomes  $1.59$  dB for  $SN = 32$ , the related difference goes up to  $1.73$  dB for  $SN = 64$ .

In Figure 8, the suppression rate of solid-state power amplifier (SSPA)-induced spectral growths of each technique was investigated for the input back off (IBO) values of  $4$  dB and  $5$  dB by obtaining the PSD curves of WOLA-OFDM signals produced with the implementation of PAPR reduction process using the SLM, GreenOFDM and DSO-SLM techniques. Along with that, the PSD curve of WOLA-OFDM signal amplified by the linear HPA, which doesn't have any disruptive effect on the signal to be amplified, was added to the same figure for comparison. In this simulation, the smoothness coefficient, which is another parameter belonging to the SSPA, was determined as  $p = 0.5$  while the search number is appointed as  $SN = 16$ . According to the Figure 8, for each IBO value, the side lobes of the WOLA-OFDM signal amplified via the SSPA were suppressed more by the DSO-SLM technique compared to the other methods. For example, while the differences of  $5.59$  dB and  $10.73$  dB occur between the side lobe level of DSO-SLM and those of the other two techniques called GreenOFDM and SLM, respectively for  $IBO = 4$  dB, the aforementioned side lobe level differences become equal to  $2.60$  dB and  $6.70$  dB



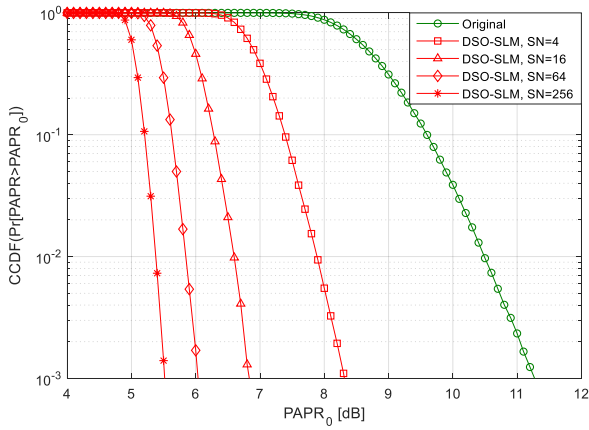


**Figure 6.** PAPR achievement of the DSO-SLM scheme for varied search numbers.

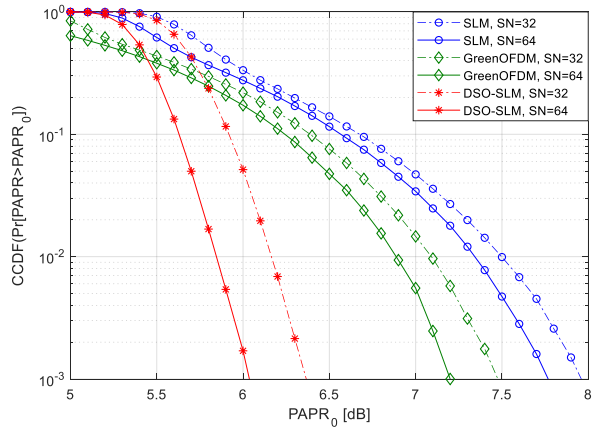


**Figure 7.** The comparative analysis of the PAPR achievements belonging to the SLM, GreenOFDM and DSO-SLM methods for different number of searches.

values for IBO = 5 dB. In Figure 9,  $PAPR_0$  [dB] – CCDF curves of DSO-PTS and DSO-SLM schemes were compared for 4, 16, 64 and 256 number of searches. As it is apparent in the Figure 9, the DSO-SLM technique demonstrates a superior PAPR reduction performance by clearly outperforming the DSO-PTS scheme in each search number. Especially in  $SN = 64$  and  $SN = 256$  search numbers, the performance difference between these two methods has become more prominent. For instance, if the PAPR values that both techniques reach at the level of  $CCDF = 10^{-3}$  for diversified search numbers are taken into consideration, the differences between the PAPR values achieved by the DSO-PTS and DSO-SLM for  $SN = 4, 16, 64$  and  $256$  search numbers are equal to 0.18 dB, 0.23 dB, 0.27 dB and 0.28 dB, respectively.

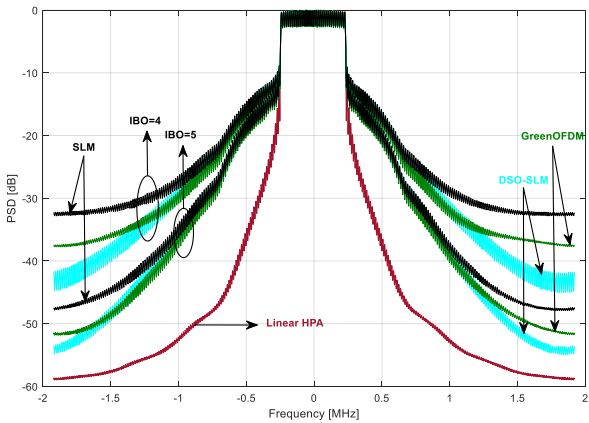


**Figure 8.** The PSD performances of SLM, GreenOFDM and DSO-SLM schemes.

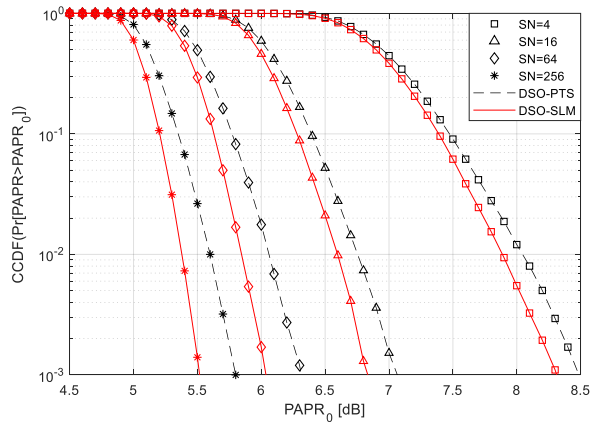


**Figure 9.** The comparison of DSO-PTS and DSO-SLM strategies in point of their PAPR achievements for assorted number of searches.

In Figure 10, the DSO-PTS and DSO-SLM techniques were compared with regard to their capabilities of suppressing the spectral growths caused by the disruptive influence of the SSPA on the signals with high PAPR. The aforementioned comparison is made for two different IBO values, 4 dB and 5 dB. If the attention is paid to the side lobe levels of the PSD curves existing in the Figure 10, it will be easily seen that the spectral growths can be suppressed more by the DSO-SLM technique, which has a superior PAPR alleviation capability compared to the DSO-PTS technique. A significant difference occurs between the side lobe levels belonging to the DSO-PTS and DSO-SLM strategies for IBO = 4 dB. When the IBO value is made equal to 5 dB, since the PSD curves of the related techniques approach to each other, the difference between the levels of PSD curves declines. For instance, the differences between the side lobe levels acquired by the DSO-PTS and DSO-SLM schemes for IBO = 4 dB and IBO = 5 dB are equal to 2.37 dB and 0.40 dB, respectively.

## 7. CONCLUSION

In this paper, the procedure of dual symbol optimization was combined with the conventional SLM scheme to prevent its performance loss caused by the symbol overlapping operation carried out in the WOLA-OFDM transmitter. Thanks to the related combination process, a new PAPR reduction strategy with the name of DSO-SLM, which is compatible with the WOLA-OFDM transmitter and resistant to the operation of symbol

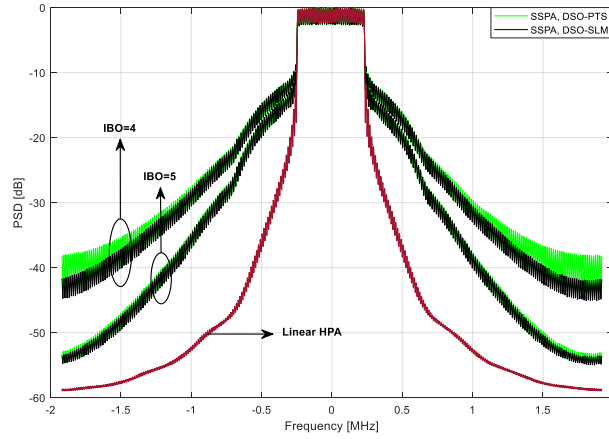


**Figure 10.** The comparison of DSO-PTS and DSO-SLM strategies in point of their PSD performances.

overlapping, was developed. In order to measure how much gain is achieved in the performance of classical SLM scheme through the aforementioned modification, the classical SLM scheme and its new modified variant called DSO-SLM were compared with regard to their PAPR and PSD achievements. On the other hand, it will never be sufficient to compare a newly developed strategy with only one scheme that is outdated like SLM. For this reason, apart from the conventional SLM, two state of art PAPR reduction methods named GreenOFDM and DSO-PTS, both of which have proven their efficiency in the literature, were also employed in the performance comparisons carried out to demonstrate the efficiency of our proposed technique. As it is proven by the PAPR and PSD graphs obtained to make performance comparisons between the DSO-SLM and the other considered methods, our proposed strategy significantly outperforms not only the conventional SLM, but also the GreenOFDM and DSO-PTS schemes.

Relying completely on the random search procedure can be considered as the main disadvantage of DSO-SLM together with the classical SLM, DSO-PTS and GreenOFDM considered as benchmark strategies in this paper. In each of these PAPR reduction strategies including the proposed one, randomly generated phase sequences are used to find the optimum phase combination providing the minimum PAPR. For this reason, high number of searches, each of which is carried out by generating and evaluating a random phase sequence, is needed to reach much better PAPR levels. On the other hand, it is possible to make DSO-SLM capable of reaching lower PAPR levels with smaller number of searches by optimizing the phase sequences via an efficient optimization algorithm instead of using the random search procedure. This opportunity can be evaluated in future studies.

## Funding

This study was supported by the Scientific Research Projects Coordination Unit of Erciyes University [Grant No: FDK-2018-8463].

## Author Contributions

**Şakir Şimşir:** Methodology, Software, Formal analysis, Writing - review & editing

**Necmi Taşpınar:** Project Administration, Funding Acquisition, Validation and Supervision

## Conflict of Interest

The authors declare that they have no conflict of interest.

## REFERENCES

- [1] M. Agiwal, A. Roy, and N. Saxena, "Next generation 5G wireless networks: a comprehensive survey," *IEEE Commun. Surv. Tutor.*, vol. 18, no. 3, pp. 1617-1655, 2016.
- [2] A. Durmuş, and Z. Yıldırım, "Design and comparative analysis of E-Shape and H-Shape microstrip patch antenna for IoT application," *J. Eng. Sci. Res.*, vol. 6, no. 1, pp. 88-97, 2024.
- [3] N. Panwar, S. Sharma, and A. K. Singh, "A survey on 5G: The next generation of mobile communication," *Phys. Commun.*, vol. 18, no. 2, pp. 64-84, 2016.
- [4] S.-Y. Lien, S.-L. Shieh, Y. Huang, B. Su, Y.-L. Hsu, and H.-Y. Wei, "5G new radio: waveform, frame structure, multiple access, and initial access," *IEEE Commun. Mag.*, vol. 55, no. 6, pp. 64-71, 2017.
- [5] Qualcomm Inc., "Waveform candidates," R1-162199, Busan, Korea, April 11-15, 2016.
- [6] R. Zayani, Y. Medjahdi, H. Shaiek, and D. Roviras, "WOLA-OFDM: a potential candidate for asynchronous 5G," *IEEE Globecom Workshops (GC Wkshps)*, pp. 1-5, Washington, 2016.
- [7] M.H.N. Shaikh, V.A. Bohara, and A. Srivastava, "Spectral analysis of a nonlinear WOLA-OFDM

- system with DPD,” National Conference on Communications (NCC), pp. 1-4, Kharagpur, 2020.
- [8] H. Shaiek, R. Zayani, Y. Medjahdi, and D. Roviras, “Analytical analysis of SER for beyond 5G post-OFDM waveforms in presence of high power amplifiers,” *IEEE Access*, vol. 7, pp. 29441-29452, 2019.
- [9] H.G. Ryu, J.S. Park, and J.S. Park, “Threshold IBO of HPA in the predistorted OFDM communication system,” *IEEE Trans. Broadcast.*, vol. 50, no. 4, pp. 425-428, 2004.
- [10] M.C.P. Paredes, F. Grijalva, J.C. Rodrigez, and F. Sarzosa, “Performance analysis of the effects caused by HPA models on an OFDM signal with high PAPR,” *IEEE Second Ecuador Technical Chapters Meeting (ETCM)*, pp. 1-5, Salinas, 2017.
- [11] Y. Rahmatallah, and S. Mohan, “Peak-to-average power ratio reduction in OFDM systems: A survey and taxonomy,” *IEEE Commun. Surv. Tutor.*, vol. 15, no. 4, pp. 1567-1592, 2013.
- [12] T. Jiang, and Y. Wu, “An overview: Peak-to-average power ratio reduction techniques for OFDM signals,” *IEEE Trans. Broadcast.*, vol. 54, no. 2, pp. 257-268, 2008.
- [13] R.W. Bauml, R.F. H. Fischer, and J.B. Huber, “Reducing the peak-to-average power ratio of multicarrier modulation by selected mapping,” *Electron. Lett.*, vol. 32, no. 22, pp. 2056-2057, 1996.
- [14] C.-L. Wang, and Y. Ouyang, “Low-complexity selected mapping schemes for peak-to-average power ratio reduction in OFDM systems,” *IEEE Trans. Signal Process.*, vol. 53, no. 12, pp. 4652-4660, 2005.
- [15] K. Tani, Y. Medjahdi, H. Shaiek, R. Zayani, and D. Roviras, “PAPR reduction of post-OFDM waveforms contenders for 5G & beyond using SLM and TR algorithms,” *25th International Conference on Telecommunications (ICT)*, pp. 104-109, Saint-Malo, 2018.
- [16] R. Zayani, H. Shaiek, X. Cheng, X. Fu, C. Alexandre, and D. Roviras, “Experimental testbed of post-OFDM waveforms toward future wireless networks,” *IEEE Access*, vol. 6, pp. 67665-67680, 2018.
- [17] N. Taşpınar, and Ş. Şimşir, “Dual symbol optimization-based partial transmit sequence technique for PAPR reduction in WOLA-OFDM waveform,” *Int. J. Commun. Syst.*, vol. 32, no. 14, pp. 1-16, 2019.
- [18] D.J.G. Mestdagh, J.L.G. Monsalve, and J.-M. Brossier, “GreenOFDM: a new selected mapping method for OFDM PAPR reduction,” *Electron. Lett.*, vol. 54, no. 7, pp. 449-450, 2018.
- [19] C. Tellambura, “Computation of the continuous-time PAR of an OFDM signal with BPSK subcarriers,” *IEEE Commun. Lett.*, vol. 5, no. 5, pp. 185-187, 2001.
- [20] A.V. Oppenheim, R.W. Schaffer, and J.R. Buck, “Discrete-Time Signal Processing,” New Jersey: Prentice Hall, 1999.